RUNX1 inhibits proliferation and induces apoptosis of t(8;21) leukemia cells *via* KLF4-mediated transactivation of P57

Shuang Liu,[1*] Yanyan Xing,[1*] Wenting Lu,[1] Shouyun Li,[1] Zheng Tian,[1] Haiyan Xing,[1] Kejing Tang,[1] Yingxi Xu,[1] Qing Rao,[1] Min Wang[1] and Jianxiang Wang[1,2]

These authors contributed equally to this work.

[1]State Key Laboratory of Experimental Hematology and [2]National Clinical Research Center for Blood Diseases, Institute of Hematology and Blood Diseases Hospital, Chinese Academy of Medical Sciences and Peking Union Medical College, Tianjin, P.R. China

 doi:10.3324/haematol.2018.192773

Received: March 5, 2018.

Accepted: February 20, 2019.

Pre-published: February 21, 2019.

Correspondence: *JIANXIANG WANG* - wangjx@ihcams.ac.cn

MIN WANG - wangjxm@ihcams.ac.cn

Supplementary Data

Supplementary Materials

Plasmids construction

KLF4 and P57 promoter fragments containing putative RUNX1 and KLF4 binding sites were cloned from human genomic DNA by PCR with the primers listed in Supplementary Table. The amplified fragments were then inserted into the pGL3-Basic vector (Promega, USA) and named as pGL3-KLF4 and pGL3-P57, respectively.

KLF4 target genes reporter plasmid (KLF4-Reporter) was constructed by inserting four tandem-linked response elements of KLF4 (AGGGTGTGGCC) into the pGL3-Basic vector through KpnI and Bgl II restriction enzyme digestion sites.

The pCMV5-RUNX1, pCMV5-RUNX1-ETO and pCMV5-KLF4 plasmids were preserved by our laboratory. Full-length and different truncation mutants of RUNX1 and RUNX1-ETO were cloned from pCMV5-RUNX1 and pCMV5-RUNX1-ETO plasmids and inserted into the pCMV5-vector with the primers listed in Supplementary Table. Lentiviral vectors used in this study were constructed by cloning the open reading frame of RUNX1, KLF4 and P57 respectively into the pCDH-EF1-MCS-T2A-copGFP vector (System Biosciences, Mountain View, CA) with primers listed in Supplementary Table.

Lentiviral preparation and transduction of Kasumi-1 cells and HL-60 cells

Lentiviral vectors were co-transfected with packaging vectors psPAX2 and pMD2.G into HEK293T cells using polyethylenimine (PEI) (Polysciences, Warrington,

PA, USA) to produce lentivirus. At 24h and 48h after transfection, viral supernatants were collected and concentrated to 100-fold by ultracentrifugation after pelleting cell debris. Then Kasumi-1 cells and HL-60 cells were transduced overnight with concentrated virus in the presence of polybrene (Sigma, USA) at a final concentration of 8 μg/mL.

RNA isolation and real-time quantitative PCR (qRT-PCR)

RNA was extracted using RNAiso Plus (Takara, Japan) and reverse-transcribed into cDNA using M-MLV Reverse Transcriptase (Life technologies, USA). qRT-PCR analysis was performed on a 7500 Real-Time PCR system (Applied Biosystems, USA) with SYBR Green PCR kit (Takara, Japan) following the manufacturer's instructions. Primers for *RUNX1*, *KLF4* and *P57* were listed in Supplementary Table.

Western blot assay

Western blot assays were performed as previously described [1] with the following primary antibodies: RUNX1 (Abcam, ab54869, USA); KLF4 (CST, #12173, USA); KLF4 (Abcam, ab151733, USA)，P57 (CST, #2557, USA); ETO (Abcam, ab124269, USA); FLAG (Sigma, F3165, USA); MYC (CST, #2276, USA); ACTIN (Sigma, A1978, USA) and H3 (Abcam, ab61251, USA).

MTS assay

GFP^+ Kasumi-1 cells and HL-60 cells were sorted by flow cytometry at 72h after lentivirus infection. Then cell proliferation ability was measured by MTS assay as previously described [1].

Cell cycle analysis

After 72h of lentivirus infection, GFP^+ cells were sorted by flow cytometry and cell cycle analyses were performed as previously described [1]. Cell cycle distribution was calculated by ModFit software.

Apoptosis assessment by Annexin V staining and morphological analysis

At 48h and 72h after lentivirus infection, 1×10^6 cells were collected, washed with 1×AnnexinV binding buffer twice and stained with Annexin V-Alexa Fluor 647-A and PI (Biolegend, USA) according to the manufacturer's instructions. Apoptosis assay was performed with flow cytometry (Canto II, BD, USA) and Annexin V^+ cells in GFP^+ population were calculated. For morphological analysis, cytospins of GFP^+ cells were prepared at different time after flow sorting and stained with Wright-Giemsa solution. Then the morphological images were captured using a Nikon Eclipse 50i microscope (Nikon Inc., Melville, NY, USA).

Cell differentiation analysis

At 48h and 72h after lentivirus infection, 1×10^6 cells were collected and stained with the following antibodies: APC-CD11b (Biolegend, USA), PE-CD15 (Biolegend, USA) or the relative isotype controls. Then the percentage of $CD11b^+$ and $CD15^+$ cells in GFP^+ population were determined by flow cytometry (Canto II, BD, USA).

References

1. Liu S, Lu W, Li S, Li S, Liu J, Xing Y, et al. Identification of JL1037 as a novel,

specific, reversible lysine-specific demethylase 1 inhibitor that induce apoptosis and autophagy of AML cells. Oncotarget. 2017 Mar 29; 8(19):31901-31914.

Supplementary Table

Lists of primers used in this study

Primer name	Sequence 5'—3'	Use
KLF4_promoter_Bgl II_fwd	GGAAGATCTGTGACATAATAATGGTGGCT	construction of pGL3-KLF4
KLF4_promoter_Bgl II_rev	GGAAGATCTTGGGCCGGGCCGTGACGC	construction of pGL3-KLF4
P57_promoter_Kpn I_fwd	CGGGGTACCTTACCCAGTACAACAGCTT	construction of pGL3-P57
P57_promoter_Bgl II_rev	GGAAGATCTAGAGGACAGCGAGAAGAA	construction of pGL3-P57
RHD_EcoR I_fwd	CCGGAATTCGCCACCATGGACCGCAGCATGGTGGAGGTGC	construction of pCMV5-RHD-myc
RHD_BamH I_rev	CGCGGATCCTTACAGATCCTCTTCTGAGATGAGTTTTTGTTCGTTTCTGCCGATGTCTTCG	construction of pCMV5-RHD-myc
RUNX1 full-length_Bgl II_fwd	GGAAGATCTGCCACCATGGCTTCAGACAGCATA	construction of pCMV5-RUNX1-myc
RUNX1 full-length_Cla I_rev	CCATCGATTTACAGATCCTCTTCTGAGATGAGTTTTTGTTCGTAGGGCCTCCACACGGCCT	construction of pCMV5-RUNX1-myc
RUNX1△RHD_N terminal_Bgl II_fwd	GGAAGATCTGCCACCATGGCTTCAGACAGCATA	construction of pCMV5-RUNX1△RHD-myc
RUNX1△RHD_N terminal_rev	GGGCTTGGTCTGATCATCTAGGCCGCTCCTCAGCTTGCCG	construction of pCMV5-RUNX1△RHD-myc
RUNX1△RHD_C terminal_fwd	CGGCAAGCTGAGGAGCGGCCTAGATGATCAGACCAAGCCC	construction of pCMV5-RUNX1△RHD-myc
RUNX1△RHD_C terminal_Cla I_rev	CCATCGATTTACAGATCCTCTTCTGAGATGAGTTTTTGTTCGTAGGGCCTCCACACGGCCT	construction of pCMV5-RUNX1△RHD-myc
RUNX1△RHD_overlap_Bgl II_fwd	GGAAGATCTGCCACCATGGCTTCAGACAGCATA	construction of pCMV5-RUNX1△RHD-myc
RUNX1△RHD_overlap_Cla I_rev	CCATCGATTTACAGATCCTCTTCTGAGATGAGTTTTTGTTCGTAGGGCCTCCACACGGCCT	construction of pCMV5-RUNX1△RHD-myc
RUNX1-ETO full-length_Kpn I_fwd	CGGGGTACCGCCACCATGCGTATCCCCGTAGATGC	construction of pCMV5-RUNX1-ETO-myc
RUNX1-ETO full-length_Xba I_rev	TGCTCTAGATTACAGATCCTCTTCTGAGATGAGTTTTTGTTCGCGAGGGGTTGTCTCTATGG	construction of pCMV5-RUNX1-ETO-myc
RUNX1-ETO△RHD_N terminal_Kpn I_fwd	CGGGGTACCGCCACCATGCGTATCCCCGTAGATGC	construction of pCMV5-RUNX1-ETO△RHD-myc
RUNX1-ETO△RHD_N terminal_rev	GAGTGCTTCTCAGTACGATTGCCGCTCCTCAGCTTGCCGG	construction of pCMV5-RUNX1-ETO△RHD-myc
RUNX1-ETO△RHD_C terminal_fwd	CCGGCAAGCTGAGGAGCGGCAATCGTACTGAGAAGCACTC	construction of pCMV5-RUNX1-ETO△RHD-myc
RUNX1-ETO△RHD_C terminal_Xba I_rev	TGCTCTAGATTACAGATCCTCTTCTGAGATGAGTTTTTGTTCGCGAGGGGTTGTCTCTATGG	construction of pCMV5-RUNX1-ETO△RHD-myc
RUNX1-ETO△RHD_overlap_Kpn I_fwd	CGGGGTACCGCCACCATGCGTATCCCCGTAGATGC	construction of pCMV5-RUNX1-ETO△RHD-myc
RUNX1-ETO△RHD_overlap_Xba I_rev	TGCTCTAGATTACAGATCCTCTTCTGAGATGAGTTTTTGTTCGCGAGGGGTTGTCTCTATGG	construction of pCMV5-RUNX1-ETO△RHD-myc
KLF4_EcoR I_fwd	CCGGAATTCGCCACCATGAGGCAGCCACCTGGCGA	construction of pCMV5-KLF4-flag
KLF4_BamH I_rev	CGCGGATCCTTACTTATCGTCGTCATCCTTGTAATCAAAATGCCTCTTCATGTG	construction of pCMV5-KLF4-flag
RUNX1_EcoR I_fwd	CCGGAATTCGCCACCATGGCTTCAGACAGCATATT	construction of pCDH-EF1-RUNX1-myc-T2A-copGFP
RUNX1_Not I_rev	ATAAGAATGCGGCCGCCAGATCCTCTTCTGAGATGAGTTTT	construction of pCDH-EF1-RUNX1-myc-T2A-copGFP
KLF4_EcoR I_fwd	CCGGAATTCGCCACCATGAGGCAGCCACCT	construction of pCDH-EF1-KLF4-flag-T2A-copGFP
KLF4_BamH I_rev	CGCGGATCCCTTATCGTCGTCATCCTTGTAATCAAAATGCCTCTTCATG	construction of pCDH-EF1-KLF4-flag-T2A-copGFP
P57_EcoR I_fwd	CCGGAATTCGCCACCATGTCCGACGCGTCCCTCC	construction of pCDH-EF1-P57-myc-T2A-copGFP
P57_BamH I_rev	CGCGGATCCCAGATCCTCTTCTGAGATGAGTTTTTGTTCCCGCAGCCTCTTGCGCGG	construction of pCDH-EF1-P57-myc-T2A-copGFP
RUNX1_fwd	ACCGACAGCCCCAACTTCCT	qRT-PCR
RUNX1_rev	GCTTTTCCCTCTTCCACTTC	qRT-PCR
KLF4_fwd	CAAGTCCCGCCGCTCCATTACCAA	qRT-PCR
KLF4_rev	CCACAGCCGTCCCAGTCACAGTGG	qRT-PCR
P57_fwd	CTGACCAGCTGCACTCGGGGATTTC	qRT-PCR
P57_rev	GCCGCCGGTTGCTGCTACATGA	qRT-PCR
GAPDH_fwd	GAAGGTGAAGGTCGGAGTC	qRT-PCR
GAPDH_rev	GAAGATGGTGATGGGATTTC	qRT-PCR
R1_fwd	TGGTGGCTTTCCAATTCTTCT	ChIP-PCR
R1_rev	AAAGCCAAAGTCCCTCACCC	ChIP-PCR
R2_fwd	GTGGTGAGTTTCCCATGCAG	ChIP-PCR
R2_rev	TGGGGGATGAGAGTGTTTTGG	ChIP-PCR
R3_fwd	GAAGTCACACTCAAGGGCGT	ChIP-PCR
R3_rev	ACCTGTTTGAACCCTGCGAT	ChIP-PCR
R4_fwd	AAGTGGAAAGGAGAGTGCGT	ChIP-PCR
R4_rev	CACGACGCCGGCTAATTTTT	ChIP-PCR
R5_fwd	TGAGCCCTTTCACTCCCTTTC	ChIP-PCR
R5_rev	AGCCTCAAGAGAAGGCCAGA	ChIP-PCR
R6_fwd	TAATCGCGCTCTTCTCCAGC	ChIP-PCR
R6_rev	CCGTACTCACCGCCATTGTC	ChIP-PCR
R7_fwd	not suitable	ChIP-PCR
R7_rev	not suitable	ChIP-PCR

Supplementary Figure

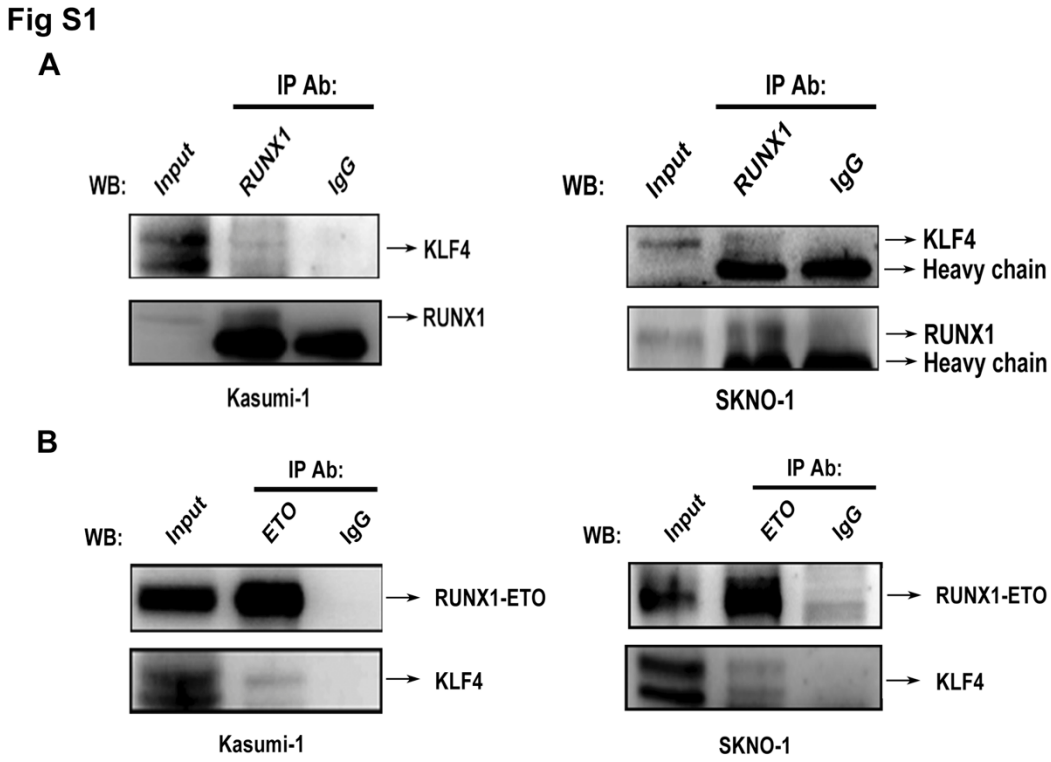

Figure S1 Endogenous interaction between KLF4 and RUNX1/ RUNX1-ETO

(A) KLF4 interacted with RUNX1 in Kasumi-1 and SKNO-1 cells. Endogenous interaction analysis of KLF4 and RUNX1 in Kasumi-1 and SKNO-1 cells with anti-RUNX1 (IP) and anti-KLF4 (IB) antibodies. **(B)** KLF4 interacted with RUNX1-ETO in Kasumi-1 and SKNO-1 cells. Endogenous interaction analysis of KLF4 and RUNX1-ETO in Kasumi-1 and SKNO-1 cells with anti-ETO (IP) and anti-KLF4 (IB) antibodies.

Fig S2

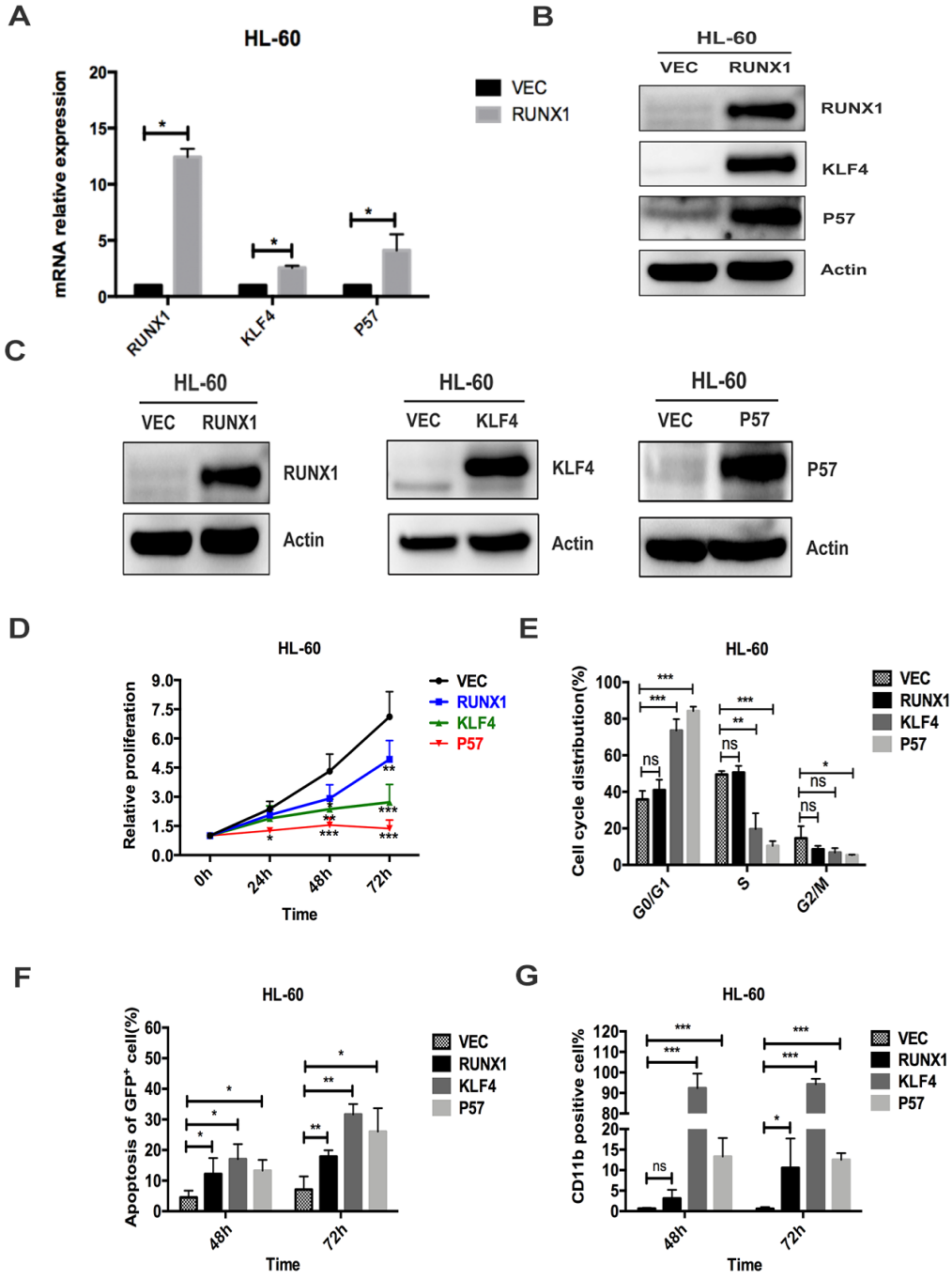

Figure S2 The biological effects of RUNX1, KLF4 and P57 overexpression on HL-60 cell proliferation, apoptosis and differentiation

(A and B) Overexpression of RUNX1 in HL-60 cells were mediated by a pCDH lentivirus system. At 72h after infection, the infected cells were sorted by flow

cytometry for GFP$^+$ population and the expression levels of RUNX1 and target genes KLF4 and P57 were measured by qRT-PCR (A) and Western blot (B), respectively. **(C)** HL-60 cells were infected with pCDH lentivirus overexpressing RUNX1, KLF4 or P57, respectively. At 72h after infection, the infected cells were sorted by flow cytometry for GFP$^+$ population and the overexpression efficiency was evaluated by Western blot assay. **(D)** MTS assay was performed to evaluate cell proliferation ability of GFP$^+$ HL-60 cells overexpressing RUNX1, KLF4 or P57 at 72h after lentivirus infection. **(E)** Cell cycle distribution of GFP$^+$ HL-60 cells overexpressing RUNX1, KLF4 or P57 was analyzed by flow cytometry with PI staining at 48h after cell sorting. **(F)** Cell apoptosis analysis of GFP$^+$ HL-60 cells overexpressing RUNX1, KLF4 or P57 were performed by the flow cytometry at 48h and 72h after lentivirus infection. **(G)** Flow cytometry analysis of cell surface markers CD11b of GFP$^+$ HL-60 cells overexpressing RUNX1, KLF4 or P57 at 48h and 72h after lentivirus infection.

Fig S3

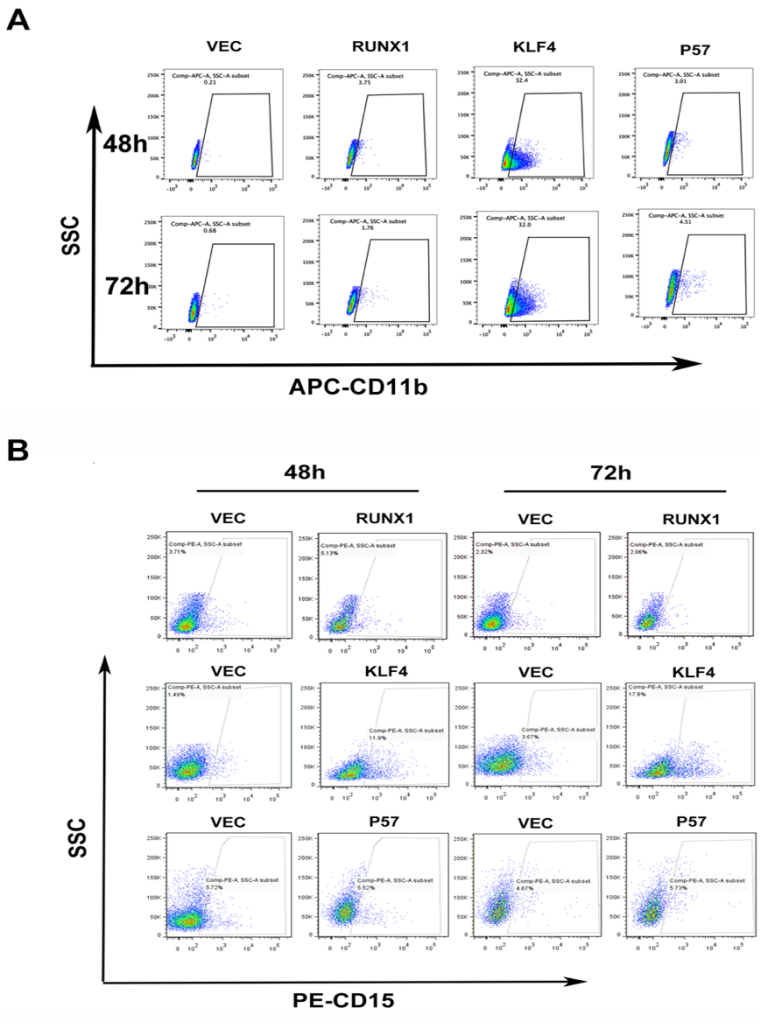

Figure S3 Representative flow cytometry plots of Kasumi-1 cell differentiation

(A) CD11b representative flow cytometry plots of GFP^+ Kasumi-1 cells overexpressing RUNX1, KLF4 or P57 at 48h and 72h after lentivirus infection. **(B)** CD15 representative flow cytometry plots of GFP^+ Kasumi-1 cells overexpressing RUNX1, KLF4 or P57 at 48h and 72h after lentivirus infection.